


P-glycoprotein (MDR1/ABCB1) restricts brain accumulation and cytochrome P450-3A (CYP3A) limits oral availability of the novel ALK/ROS1 inhibitor lorlatinib

Wenlong Li¹, Rolf W. Sparidans², Yaogeng Wang¹, Maria C. Lebre¹, Els Wagenaar¹, Jos H. Beijnen^{1,2,3} and Alfred H. Schinkel ¹

¹ Division of Pharmacology, The Netherlands Cancer Institute, Plesmanlaan 121, 1066 CX, Amsterdam, The Netherlands

² Faculty of Science, Department of Pharmaceutical Sciences, Division of Pharmacoepidemiology & Clinical Pharmacology, Utrecht University, Universiteitsweg 99, 3584 CG, Utrecht, The Netherlands

³ Department of Pharmacy & Pharmacology, The Netherlands Cancer Institute/Slotervaart Hospital, Plesmanlaan 121, 1066 CX, Amsterdam, The Netherlands

Lorlatinib (PF-06463922) is a promising oral anaplastic lymphoma kinase (ALK) and ROS1 inhibitor currently in Phase III clinical trials for treatment of non-small-cell lung cancer (NSCLC) containing an ALK rearrangement. With therapy-resistant brain metastases a major concern in NSCLC, lorlatinib was designed to have high membrane and blood–brain barrier permeability. We investigated the roles of the multidrug efflux transporters ABCB1 and ABCG2, and the multispecific drug-metabolizing enzyme CYP3A in plasma pharmacokinetics and tissue distribution of lorlatinib using genetically modified mouse strains. *In vitro*, human ABCB1 and mouse *Abcg2* modestly transported lorlatinib. Following oral lorlatinib administration (at 10 mg/kg), brain accumulation of lorlatinib, while relatively high in wild-type mice, was still fourfold increased in *Abcb1a/1b*^{-/-} and *Abcb1a/1b;Abcg2*^{-/-} mice, but not in single *Abcg2*^{-/-} mice. Lorlatinib plasma levels were not altered. Oral coadministration of the ABCB1/ABCG2 inhibitor elacridar increased the brain accumulation of lorlatinib in wild-type mice fourfold, that is, to the same level as in *Abcb1a/1b;Abcg2*^{-/-} mice, without altering plasma exposure. Similar results were obtained for lorlatinib testis accumulation. In *Cyp3a*^{-/-} mice, the plasma exposure of lorlatinib was increased 1.3-fold, but was then twofold reduced upon transgenic overexpression of human CYP3A4 in liver and intestine, whereas relative tissue distribution of lorlatinib remained unaltered. Our data indicate that lorlatinib brain accumulation is substantially limited by P-glycoprotein/ABCB1 in the blood–brain barrier, but this can be effectively reversed by elacridar coadministration. Moreover, oral availability of lorlatinib is markedly restricted by CYP3A4 activity. These insights may be used in optimizing the therapeutic application of lorlatinib.

Lung cancer is one of the most common and lethal malignancies, with about 234,000 new cases and 154,000 deaths expected to occur in the USA alone in 2018, accounting for about 13% of new cancers and 25% of cancer mortality.¹ Most lung cancers (~90%) are non-small-cell lung cancers (NSCLCs), consisting of a number of subtypes driven by

various activated oncogenes.^{2,3} Activating gene rearrangements in anaplastic lymphoma kinase (ALK+) have been shown to be oncogenic drivers in 3–7% of patients with NSCLC and other cancers.⁴ As the ALK rearrangement presents a promising molecular target for treatment, several ALK inhibitors have been developed.

Key words: lorlatinib, P-glycoprotein, brain accumulation, cytochrome P450-3A, oral availability

Abbreviations: ABC: ATP-binding cassette; ALK: anaplastic lymphoma kinase; ANOVA: analysis of variance; AUC: area under plasma concentration–time curve; BCRP: breast cancer resistance protein; C_{brain} : brain concentration; C_{max} : maximum drug concentration in plasma; C_{testis} : testis concentration; CNS: central nervous system; CYP: cytochrome P450; *Cyp3aXAV*: *Cyp3a* knockout mice with specific expression of human CYP3A4 in liver and intestine; EML4: echinoderm microtubule associated protein-like 4; h (as prefix): human; LC-MS/MS: liquid chromatography coupled with tandem mass spectrometry; MDCK: Madin-Darby canine kidney; m (as prefix): mouse; NSCLC: non-small-cell lung cancer; P_{brain} : relative brain accumulation; P_{testis} : relative testis accumulation; P-gp: P-glycoprotein; SD: standard deviation; TKI: tyrosine kinase inhibitor; T_{max} : time to reach maximum drug concentration in plasma

Additional Supporting Information may be found in the online version of this article.

Conflict of Interest: The research group of Alfred H. Schinkel receives revenue from commercial distribution of some of the mouse strains used in this study.

Grant sponsor: China Scholarship Council (CSC Scholarship No.201606220081)

DOI: 10.1002/ijc.31582

History: Received 24 Feb 2018; Accepted 20 Apr 2018; Online 9 May 2018

Correspondence to: Alfred H. Schinkel, Division of Pharmacology, The Netherlands Cancer Institute, Plesmanlaan 121, 1066 CX Amsterdam, The Netherlands, Tel.: +31-20-512-2046, Fax: +31-20-512-1792, E-mail: a.schinkel@nki.nl

What's new?

Lorlatinib, a high-affinity inhibitor of oncogenic receptor tyrosine kinases ALK and ROS1, is under clinical study for the treatment of non-small-cell lung cancer (NSCLC). Because lorlatinib accumulates in the brain, it could be effective against brain metastases, which limit the efficacy of most other NSCLC drugs. In this investigation, lorlatinib was found to interact with the ATP-binding cassette (ABC) drug efflux transporters P-glycoprotein/ABCB1, which markedly restricted lorlatinib brain penetration. While pharmacological inhibition of ABCB1 reversed these effects, lorlatinib oral availability was further clearly restricted by CYP3A-mediated metabolism. The findings could help facilitate the clinical development of lorlatinib.

Crizotinib, the first-generation ALK inhibitor, was approved by the FDA in 2011 for metastatic NSCLC. Although crizotinib demonstrates initial robust efficacy in ALK-positive tumors, they typically become resistant through development of secondary resistance mutations in ALK or disease progression in the brain.^{5,6} Many lung cancer patients have brain metastases and a poor prognosis, which may be due in part to the poor blood-brain barrier (BBB) permeability of most drugs. The second-generation ALK inhibitor ceritinib was initially prescribed only for crizotinib-resistant metastatic disease, but it is now also used to treat primary ALK-positive lung cancer.^{7,8}

To optimize third-generation ALK inhibitors, substantial effort has been put into developing a small-molecule inhibitor that combined good central nervous system (CNS) penetration with broad-spectrum ALK potency. These properties could have potential utility in the treatment of patients who exhibit both resistance mutations and brain metastases. Utilizing structured drug design, a unique macrocyclic ALK inhibitor, lorlatinib (PF-06463922, Supporting Information, Fig. 1) was developed, which possesses significantly increased lipophilicity relative to its acyclic analogs.⁹

Lorlatinib is a selective and highly potent ATP-competitive inhibitor of ALK and ROS1. Preclinical data show that it displayed superior potency relative to crizotinib, ceritinib and alectinib against all known clinically acquired ALK mutations including the highly resistant G1202R mutation, which confers resistance to the other ALK inhibitors, including brigatinib.^{10,11} Moreover, lorlatinib has high passive membrane permeability.⁹ In a first-in-man Phase I study (NCT01970865), the safety, dosing, pharmacokinetics and efficacy of lorlatinib in patients with advanced ALK-positive or ROS1-positive NSCLC were recently reported.¹² In patients in whom two or more different ALK tyrosine kinase inhibitor (TKI) treatments had failed (including a second-generation ALK TKI), a confirmed response was seen in 42% of patients and the median duration of response was 11.7 months. Moreover, lorlatinib was highly active in the CNS, inducing intracranial response in 42% and 60% of ALK-positive and ROS1-positive patients with baseline measurable CNS disease, respectively. Lorlatinib was generally well tolerated by patients, with predominantly grade 1 or 2 adverse events. The most significant treatment-related adverse effects were hypercholesterolemia and hypertriglyceridemia. No maximum tolerated dose was identified, and the recommended Phase II dose was 100 mg once daily. Interestingly, one NSCLC

patient was resensitized to crizotinib after lorlatinib failure due to a secondary ALK mutation.¹³ Lorlatinib is currently studied in Phase III clinical trials for primary treatment of advanced or metastatic lung cancer.

The ATP-binding cassette (ABC) drug efflux transporters P-glycoprotein (P-gp; ABCB1) and breast cancer resistance protein (BCRP; ABCG2) are highly expressed in the intestinal epithelium, liver and in the blood-brain barrier (BBB), as well as in a number of tumors.¹⁴⁻¹⁶ They can limit the oral availability and brain accumulation of many clinically used anticancer drugs, and can also directly confer multidrug resistance to tumor cells, which may well limit the therapeutic efficacy of these drugs, especially against brain metastases.^{17,18} It is therefore important to investigate whether lorlatinib interacts with these transporters. Lorlatinib was reported to be only slightly transported by ABCB1 *in vitro*, as demonstrated in an ABCB1-overexpressing MDCK cell line (active efflux ratio $r = 1.5$).⁹ Furthermore, P-gp overexpression in ceritinib-resistant patient-derived cells did not confer lorlatinib resistance.¹⁹ Although these studies suggest only a slight interaction of lorlatinib with ABCB1 *in vitro*, the roles of Abcb1 and Abcg2 *in vivo* in brain accumulation of lorlatinib remain unknown.

Cytochrome P450 3 A (CYP3A) is a member of the CYP superfamily and CYP enzymes are responsible for most phase I drug metabolism.²⁰ CYP3A4 and CYP3A5 are the most abundant CYP enzymes in human liver and intestine, representing 40% and 80% of the total CYP enzymes expressed in each tissue, respectively.²¹ For many drugs metabolism by CYP3A4/5 leads to inactivation or sometimes activation. The plasma exposure and bioavailability of many drugs are thus strongly affected by CYP3A4/5, which can dramatically influence the therapeutic efficacy in patients. Whether lorlatinib is significantly metabolized by CYP3A or not is currently unclear based on publicly available sources.

The primary aim of this study was to clarify the *in vivo* roles of ABCB1, ABCG2, and CYP3A in modulating oral availability and/or brain accumulation of lorlatinib, using wild-type and appropriate genetically modified mouse models as well as pharmacological inhibition of ABCB1 and ABCG2.

Material and Methods**Chemicals**

Lorlatinib was purchased from TargetMol (Boston, MA). Zosuquidar and elacridar HCl were obtained from Sequoia

Research Products (Pangbourne, United Kingdom). Ko143 was from Tocris Bioscience (Bristol, United Kingdom). Bovine Serum Albumin (BSA) Fraction V was obtained from Roche Diagnostics GmbH (Mannheim, Germany). Glucose water 5% w/v was supplied by B. Braun Medical Supplies (Melsungen, Germany). Isoflurane was purchased from Pharmachemie (Haarlem, The Netherlands) and heparin (5000 IU ml⁻¹) from Leo Pharma (Breda, The Netherlands). Other chemicals used in the lorlatinib assay were described before²² and all other chemicals and reagents were obtained from Sigma-Aldrich (Steinheim, Germany).

Cell lines and transport assays

Polarized Madin-Darby Canine Kidney (MDCK-II) cells stably transduced with human (h) ABCB1, hABCG2 or mouse (m) Abcg2 cDNA were used and cultured as described previously.^{23,24} Transepithelial transport assays were performed on microporous polycarbonate membrane filters (3.0 μm pore size, 12 mm diameter, Transwell 3402, Corning Incorporated, Kennebunk, ME). The parental and variant subclones were seeded at a density of 2.5×10^5 cells per well and cultured for 3 days to form an intact monolayer. Membrane tightness was assessed by measurement of transepithelial electrical resistance.

Where appropriate, 5 μM zosuquidar (ABCB1 inhibitor) and/or 5 μM Ko143 (ABCG2/Abcg2 inhibitor) were used during the transport experiments after preincubation with these inhibitors for 1 hr in both compartments. The transport phase was started ($t=0$) by replacing the medium in the apical or basolateral compartment with fresh DMEM including 10% (v/v) fetal bovine serum (FBS) and lorlatinib at 5 μM, as well as the appropriate inhibitor(s). Cells were kept at 37°C in 5% CO₂ during the experiment, and 50 μl aliquots were taken from the acceptor compartment at 1, 2 and 4 hr, and stored at -30°C until LC-MS/MS measurement of the concentrations of lorlatinib. Active transport was expressed using the transport ratio r , that is, the amount of apically directed drug transport divided by basolaterally directed drug translocation after 4 hr.

Animals

Mice were housed and handled according to institutional guidelines complying with Dutch and EU legislation. Wild-type, *Abcb1a/1b*^{-/-}, *Abcg2*^{-/-}, *Abcb1a/1b;Abcg2*^{-/-}, *Cyp3a*^{-/-} and *Cyp3aXAV* mice, all of a >99% FVB genetic background, were used between 10 and 15 weeks of age. Animals were kept in a temperature-controlled environment with a 12-hr light and 12-hr dark cycle and they received a standard diet (Transbreed, SDS Diets, Technilab-BMI, Someren, The Netherlands) and acidified water *ad libitum*.

Drug solutions

For oral administration, lorlatinib was dissolved in dimethyl sulfoxide (DMSO) at a concentration of 50 mg/ml and further diluted with a mixture of polysorbate 80/ethanol (1:1, v/

v), and then 5% (w/v) glucose in water to yield a concentration of 1.0 mg/ml. Final concentrations for DMSO, polysorbate 80, ethanol and glucose in the dosing solution were 2%, 1.5%, 1.5% and 4.75% (v/v/v/w), respectively. Elacridar hydrochloride was dissolved in DMSO (106 mg/ml) to get 100 mg pure elacridar per ml DMSO. The stock solution was further diluted with a mixture of polysorbate 80, ethanol and water [20:13:67, (v/v/v)] to yield a concentration of 10 mg/ml elacridar, and orally administered at a dose of 100 mg/kg body weight. All dosing solutions were prepared freshly on the day of experiment.

Plasma pharmacokinetics and organ accumulation of lorlatinib in mice

To minimize variation in absorption upon oral administration, mice were fasted for 3 hrs before lorlatinib (10 mg/kg) was administered by gavage into the stomach, using a blunt-ended needle. For the 24 hr or 8 hr experiments, tail vein blood sampling was performed at 0.5, 1, 2, 4 and 8 hr or 0.25, 0.5, 1, 2 and 4 hr time points after oral administration, respectively, using microvettes containing dipotassium-EDTA. Twenty-four or eight hours after oral administration, mice were anesthetized with isoflurane and blood was collected by cardiac puncture. Blood samples were collected in Eppendorf tubes containing heparin as an anticoagulant. The mice were then sacrificed by cervical dislocation and brain, liver, spleen, kidneys, lung and small intestine were rapidly removed. The contents of the small intestine were removed, and the tissue quickly rinsed with saline to remove any residual feces before homogenization of the tissue. Plasma was isolated from the blood by centrifugation at 9,000g for 6 min at 4°C, and the plasma fraction was collected and stored at -30°C until analysis. Brain, liver, spleen, kidneys, lung and small intestinal tissue were homogenized with 1, 3, 1, 2, 1 and 3 ml of 4% (w/v) bovine serum albumin, respectively. All samples were stored at -30°C until analysis. Relative tissue accumulation after oral administration was calculated by determining lorlatinib tissue concentration at 24 or 8 hr relative to plasma AUC_{0-24 hr} or AUC_{0-8 hr}.

Brain accumulation of lorlatinib in combination with oral elacridar

Wild-type and *Abcb1a/1b;Abcg2*^{-/-} mice were fasted for 3 hr before oral administration of either elacridar (100 mg/kg) or vehicle. Fifteen minutes later, lorlatinib (10 mg/kg) was administered to mice orally. Tail vein blood sampling was performed at 7.5, 15, 30 min and 1 hr time points after lorlatinib administration. Blood, brain, liver, lung and testis were isolated at the 2 hr time point, and processed as described above. Testis was homogenized with 1 ml of 4% (w/v) bovine serum albumin. Tissue-to-plasma ratios at $t=2$ hr were calculated per individual mouse by dividing the tissue concentration by the corresponding plasma concentration.

LC-MS/MS analysis

Lorlatinib concentrations in DMEM cell culture medium, plasma samples and organ homogenates were determined using a sensitive and specific liquid chromatography-tandem mass spectrometry assay.²²

Pharmacokinetic calculations and statistical analysis

Pharmacokinetic parameters were calculated by noncompartmental methods using the software GraphPad Prism7 (GraphPad Software, La Jolla, CA). The area under the plasma concentration–time curve (AUC) was calculated using the trapezoidal rule, without extrapolating to infinity. The peak plasma concentration (C_{max}) and the time of maximum plasma concentration (T_{max}) were estimated from the original data. One-way analysis of variance (ANOVA) was used when multiple groups were compared and the Bonferroni *post hoc* correction was used to accommodate multiple testing. The two-sided unpaired Student's *t* test was used when treatments or differences between two groups were compared. Differences were considered statistically significant when $p < 0.05$. All data are presented as geometric mean \pm SD.

Results

In vitro transport of lorlatinib

Transepithelial drug transport was tested using polarized monolayers of Madin-Darby Canine Kidney (MDCK-II) parental cells and its subclones overexpressing hABCB1, hABCG2 or mAbcg2. In the parental cells there was no net transport of lorlatinib ($r = 0.92$, Fig. 1a), which was also not affected by addition of the ABCB1 inhibitor zosuquidar ($r = 0.87$, Fig. 1b). In cells overexpressing hABCB1, there was clear apically directed transport of lorlatinib ($r = 1.93$, Fig. 1c), which was completely inhibited by zosuquidar at 5 μ M ($r = 1.06$, Fig. 1d).

Zosuquidar was added to inhibit any possible contribution of endogenous canine ABCB1 in subsequent experiments with MDCK-II cells overexpressing hABCG2 and mAbcg2. Ko143, a specific ABCG2 inhibitor was used to inhibit the transport activity of hABCG2 and mAbcg2. mAbcg2-overexpressing MDCK-II cells could modestly transport lorlatinib ($r = 1.50$, Fig. 1g), and transport was inhibited by Ko143 ($r = 1.02$, Fig. 1h). There was no detectable polarized transport of lorlatinib in cells overexpressing hABCG2 either with zosuquidar alone or in combination with Ko143 (Figs. 1e and 1f). Lorlatinib thus is a fair transport substrate of hABCB1 and mAbcg2, but not detectably of hABCG2.

Impact of ABCB1 and ABCG2 on lorlatinib plasma pharmacokinetics and tissue disposition

To assess the possible impact of mAbcb1a/1b and mAbcg2 on oral availability and tissue disposition of lorlatinib, we performed a 24-hr pilot study in female wild-type and combination *Abcb1a/1b;Abcg2*^{-/-} mice, using oral administration of 10 mg/kg lorlatinib. As shown in Supporting Information,

Figure 2 and Table 1, plasma exposure of lorlatinib over 24 hr (AUC_{0–24 hr}) was not significantly different between wild-type and *Abcb1a/1b;Abcg2*^{-/-} mice.

Brain, liver, spleen, kidney, lung and small intestinal tissue concentrations of lorlatinib were also measured 24 hr after oral administration. We observed substantial increases in brain concentration (6.5-fold) and brain-to-plasma ratio (2.1-fold) in *Abcb1a/1b;Abcg2*^{-/-} mice compared to wild-type mice (Supporting Information, Fig. 3 and Table 1). In contrast, exposure of lorlatinib in other organs was not much altered when considering the tissue-to-plasma ratios (Supporting Information, Fig. 4). Interestingly, the brain-to-plasma ratios of lorlatinib were around 0.8 in wild-type mice, indicating relatively good penetration of lorlatinib into the brain at this time point.

To further investigate the separate and combined effects of mAbcb1a/1b and mAbcg2 on oral availability and tissue disposition of lorlatinib, a more extensive experiment was performed up till 8 hr, when plasma levels were still comparatively high. We administered lorlatinib (10 mg/kg) orally to female wild-type, *Abcb1a/1b*^{-/-}, *Abcg2*^{-/-} and *Abcb1a/1b;Abcg2*^{-/-} mice. As shown in Figure 2a and Table 1 and Supporting Information, Figure 5, lorlatinib was absorbed quickly, and there were no statistically significant differences in oral plasma AUC_{0–8 hr} between the strains. Thus, mAbcb1 and mAbcg2 do not substantially affect the oral availability of lorlatinib at this dose. In contrast, the lorlatinib brain concentrations were markedly increased by 4.5-fold and 4.7-fold in *Abcb1a/1b*^{-/-} and *Abcb1a/1b;Abcg2*^{-/-} mice, respectively, compared to wild-type mice (Fig. 3a Table 1), but not in single *Abcg2*^{-/-} mice. At 8 hr, the brain-to-plasma ratios of lorlatinib were also relatively high (0.4) in wild-type mice, and these were further increased 3.9-fold by deficiency of mAbcb1 or mAbcb1 and mAbcg2 together, but not in single *Abcg2*^{-/-} mice (Fig. 3b Table 1). Similar results were obtained for the brain accumulations (Fig. 3c Table 1). These data indicate that mAbcb1 can markedly restrict brain accumulation of lorlatinib, whereas mAbcg2 has little or no role in this process.

In contrast to brain, liver, spleen, kidney, lung and small intestinal tissue yielded no meaningful differences in tissue concentrations, tissue-to-plasma ratios or tissue accumulation of lorlatinib between the mouse strains. Tissue-to-plasma distribution ratios were about 8.0, 4.0, 1.3, 1.5 and 3.0 for liver, spleen, kidney, lung and small intestinal tissue, respectively (Supporting Information, Fig. 6), so still clearly higher than observed for the brain (0.4). As lorlatinib is a relatively hydrophobic drug, these tissue-to-plasma ratios of well above 1 for most tissues may reflect a relatively higher affinity of the drug to reside in tissue as compared to plasma, whereas abundant drug uptake systems present in the sinusoidal membrane of the liver may have further boosted lorlatinib accumulation in this organ.

Impact of CYP3A on lorlatinib plasma pharmacokinetics and tissue disposition

As CYP3A plays an important role in metabolism of many drugs, and therefore in restricting oral availability of its

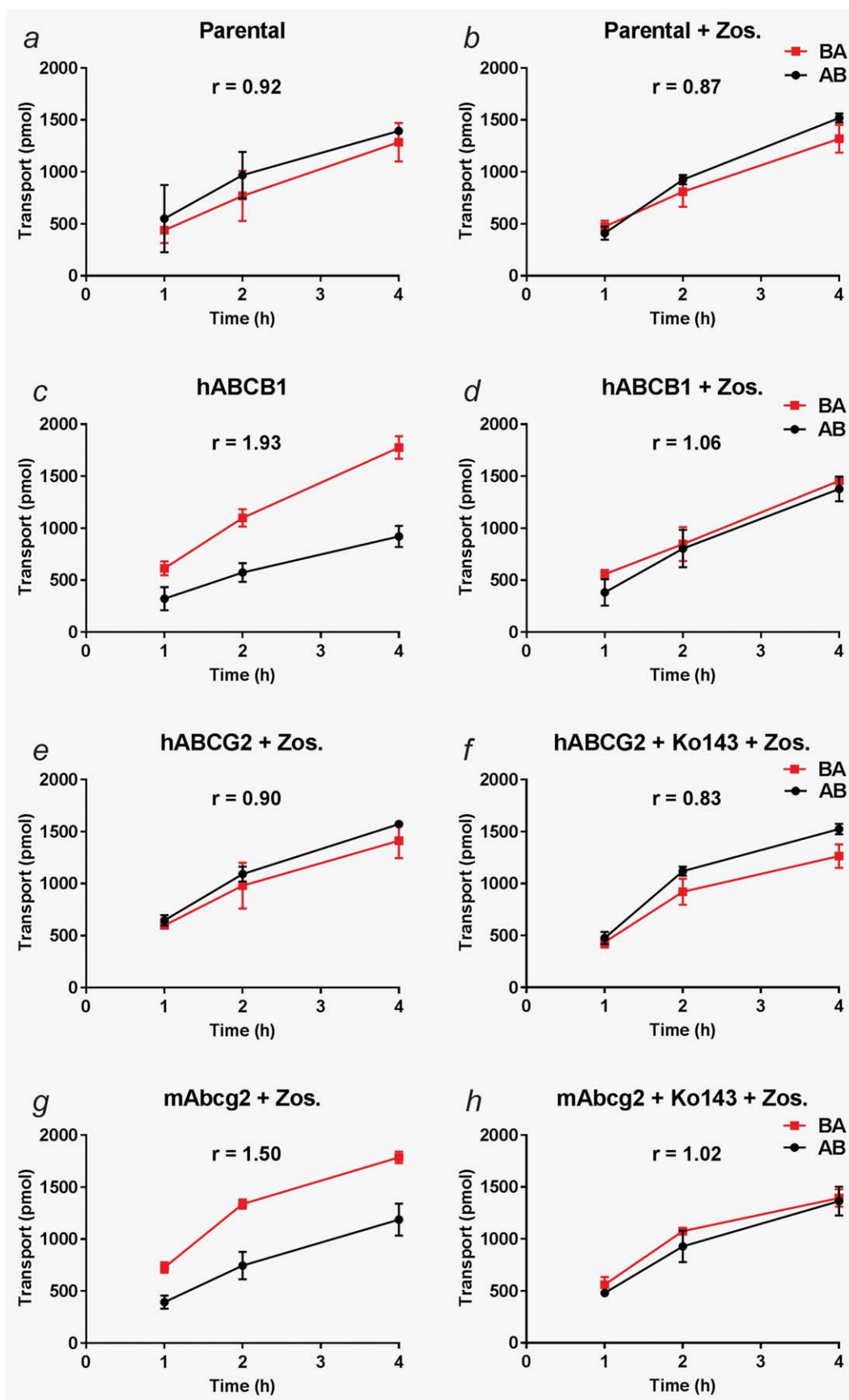


Figure 1. Transepithelial transport of lorlatinib (5 μ M) assessed in MDCK-II cells either nontransduced (a, b), transduced with hABCB1 (c, d), hABCG2 (e, f) or mAbcg2 (g, h) cDNA. At $t = 0$ hr, lorlatinib was applied in the donor compartment and the concentrations in the acceptor compartment at $t = 1, 2$ and 4 hr were measured and plotted as lorlatinib transport (pmol) in the graph ($n = 3$). (b, d–h) Zos. (zosuquidar, 5 μ M) was applied to inhibit human and/or endogenous canine ABCB1. (f, h) The ABCG2 inhibitor Ko143 (5 μ M) was applied to inhibit ABCG2/Abcg2-mediated transport. r , relative transport ratio. BA (■), translocation from the basolateral to the apical compartment; AB (●), translocation from the apical to the basolateral compartment. Points, mean; bars, SD. [Color figure can be viewed at wileyonlinelibrary.com]

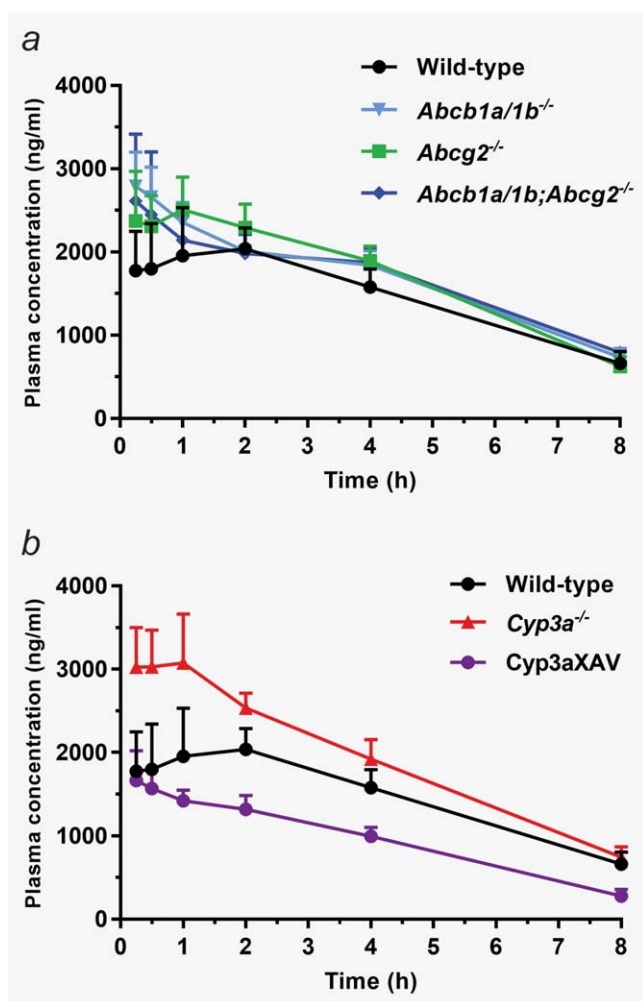


Figure 2. Plasma concentration–time curves of lorlatinib in female wild-type, *Abcb1a/1b*^{-/-}, *Abcg2*^{-/-}, *Abcb1a/1b;Abcg2*^{-/-}, *Cyp3a*^{-/-} and *Cyp3aXAV* mice over 8 hr after oral administration of 10 mg/kg lorlatinib ($n = 5–7$). Panel a: wild-type, *Abcb1a/1b*^{-/-}, *Abcg2*^{-/-} and *Abcb1a/1b;Abcg2*^{-/-} mice. Panel b: wild-type, *Cyp3a*^{-/-} and *Cyp3aXAV* mice. [Color figure can be viewed at wileyonlinelibrary.com]

substrates, an 8-hr experiment was performed to study the effect of CYP3A on lorlatinib plasma exposure. In this experiment, female wild-type, *Cyp3a* knockout (*Cyp3a*^{-/-}), and *Cyp3a*^{-/-} mice with specific transgenic expression of human CYP3A4 in liver and intestine (*Cyp3aXAV* mice) were used. After oral administration of 10 mg/kg lorlatinib, blood and organs were collected and processed as described above. The oral $AUC_{0-8 \text{ hr}}$ in *Cyp3a*^{-/-} mice was 1.3-fold higher ($p < 0.001$) than that in wild-type mice. Moreover, lorlatinib plasma exposure in *Cyp3aXAV* mice was decreased by 1.6-fold ($p < 0.001$) relative to that in wild-type mice and by 2-fold ($p < 0.001$) relative to *Cyp3a*^{-/-} mice (Fig. 2b Table 1). This clearly suggests that human CYP3A4 plays an important role in lorlatinib metabolism and oral availability.

In contrast to the marked effect on overall plasma exposure, the brain-to-plasma ratios and brain accumulations of lorlatinib were not significantly altered in *Cyp3a*^{-/-} or

Cyp3aXAV mice (Fig. 3 and Table 1). Similar minor effects were observed for liver, spleen, kidney, lung and small intestinal tissue (Supporting Information, Fig. 6), indicating no substantial impact of CYP3A on the relative tissue distribution of lorlatinib. Collectively, these results suggest that lorlatinib is substantially metabolized by mouse *Cyp3a* and human CYP3A4, which markedly affects the oral availability of lorlatinib.

Effect of the dual ABCB1 and ABCG2 inhibitor elacridar on lorlatinib brain accumulation

In view of the potential benefit of further enhancing lorlatinib brain accumulation, we wanted to assess to what extent the dual ABCB1 and ABCG2 inhibitor elacridar could modulate the bioavailability and brain accumulation of lorlatinib. For this purpose, we administered elacridar (100 mg/kg) orally 15 min prior to oral lorlatinib (10 mg/kg) to male wild-type and *Abcb1a/1b;Abcg2*^{-/-} mice, and assessed plasma and brain lorlatinib levels 2 hr later. This 2-hr time span was used to maintain sufficiently high elacridar levels in plasma throughout the experiment, ensuring complete inhibition of the BBB ABC transporters. Moreover, the lorlatinib plasma concentration was relatively high around 2 hr, making the impact of the BBB transporter proteins especially relevant. In vehicle-treated mice, lorlatinib plasma $AUC_{0-2 \text{ hr}}$ were not different between wild-type and *Abcb1a/1b;Abcg2*^{-/-} mice, and pretreatment with elacridar did not result in significant further alterations (Supporting Information, Fig. 7). These results indicate that lorlatinib plasma exposure and oral availability are not significantly affected by the presence of elacridar, which is in line with what we previously observed for the genetic knockout of *Abcb1a/1b* and *Abcg2* (Fig. 2a).

In the absence of elacridar, brain concentrations of lorlatinib were 3.8-fold higher in *Abcb1a/1b;Abcg2*^{-/-} mice than in wild-type mice (Fig. 4a Table 2). In contrast to the minor effects on plasma exposure, elacridar substantially increased the brain concentrations, brain-to-plasma ratios and brain accumulation of lorlatinib in wild-type mice by 3.8-fold, 3.8-fold and 4.0-fold, respectively (all $p < 0.001$), resulting in levels similar to those observed in *Abcb1a/1b;Abcg2*^{-/-} mice with or without elacridar (Figs. 4ac Table 2). In contrast, elacridar did not significantly affect these parameters in *Abcb1a/1b;Abcg2*^{-/-} mice (Figs. 4a–4c), further supporting that the pharmacokinetic effect of elacridar was specifically mediated by inhibition of the ABC transporters in the BBB.

As testis resembles the brain with respect to the presence of ABCB1 and ABCG2 in the blood–testis barrier (BTB), this organ was also analyzed to assess whether lorlatinib is kept out by ABCB1 and ABCG2 in the BTB. As shown in Figure 4e, in the absence of elacridar, testis-to-plasma ratios of lorlatinib were 2.5-fold higher in *Abcb1a/1b;Abcg2*^{-/-} mice than in wild-type mice. Elacridar coadministration resulted in a pronounced increase in testis concentrations (2.9-fold) and testis-to-plasma ratios (2.9-fold) of lorlatinib in wild-type mice to levels equal to those in *Abcb1a/1b;Abcg2*^{-/-} mice

Table 1. Plasma and brain pharmacokinetic parameters of lorlatinib 8 hr after oral administration of 10 mg/kg lorlatinib to female wild-type, *Abcb1a/1b*^{-/-}, *Abcg2*^{-/-}, *Abcb1a/1b;Abcg2*^{-/-}, *Cyp3a*^{-/-} and *Cyp3aXAV* mice

Parameter	Genotype					
	Wild-type	<i>Abcb1a/1b</i> ^{-/-}	<i>Abcg2</i> ^{-/-}	<i>Abcb1a/1b;Abcg2</i> ^{-/-}	<i>Cyp3a</i> ^{-/-}	<i>Cyp3aXAV</i>
AUC _{0-8h} , ng/ml hr	11,701 ± 1,274	13,470 ± 1,267	13,706 ± 1,260	13,346 ± 1,086	15,257 ± 1,342***	7,585 ± 533***, ###
Fold change AUC _{0-8 hr}	1.0	1.2	1.2	1.1	1.3	0.6
C _{max} , ng/ml	2,138 ± 440	2,806 ± 420	2,592 ± 433	2,710 ± 656	3,272 ± 449	1,711 ± 309
T _{max} , hr	2.0	0.25	1.0	0.25	1.0	0.25
C _{brain} , ng/g	299 ± 58	1,334 ± 307***	335 ± 126	1,407 ± 271***	331 ± 53	170 ± 33
Fold change C _{brain}	1.0	4.5	1.1	4.7	1.1	0.6
Brain-to-plasma ratio	0.46 ± 0.09	1.81 ± 0.27***	0.53 ± 0.11	1.80 ± 0.43***	0.46 ± 0.06	0.65 ± 0.14
Fold change ratio	1.0	3.9	1.2	3.9	1.0	1.4
P _{brain} (×10 ⁻³ hr ⁻¹)	25.6 ± 4.5	99.0 ± 19.6***	25.1 ± 12.1	105.0 ± 13.7***	21.9 ± 4.1	22.4 ± 4.0
Fold change P _{brain}	1.0	3.9	1.0	4.1	0.9	0.9

Abbreviations: AUC_{0-8 hr}, area under plasma concentration-time curve; C_{max}, maximum concentration in plasma; T_{max}, time point (h) of maximum plasma concentration; C_{brain}, brain concentration; P_{brain}, relative brain accumulation, calculated by determining the lorlatinib brain concentration relative to the AUC_{0-8 hr}.

p* < 0.05; *p* < 0.01; ****p* < 0.001 compared to wild-type mice.

#*p* < 0.05; ##*p* < 0.01; ###*p* < 0.001 comparing *Cyp3a*^{-/-} and *Cyp3aXAV* mice.

Data are presented as mean ± SD (*n* = 5–7).

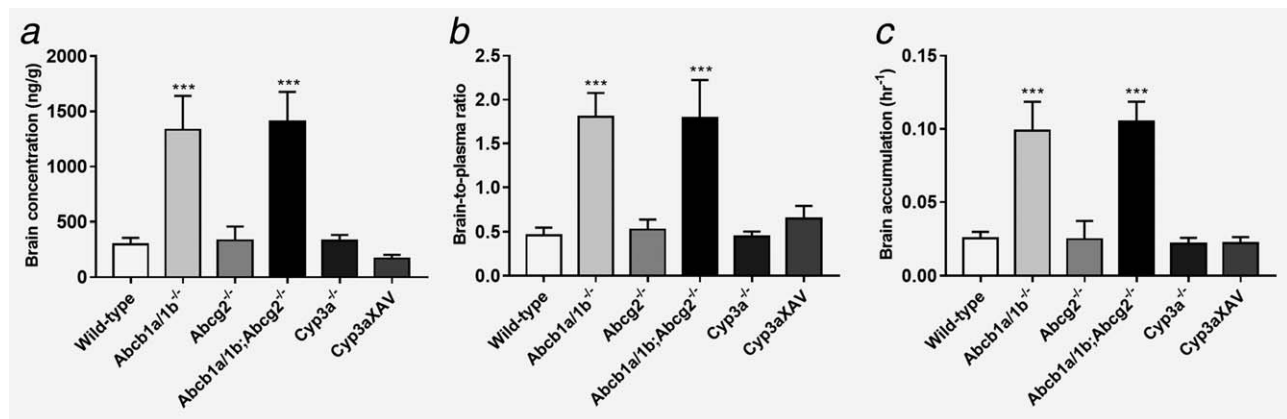


Figure 3. Brain concentration (a), brain-to-plasma ratio (b) and brain accumulation (c) of lorlatinib in female wild-type, *Abcb1a/1b*^{-/-}, *Abcg2*^{-/-}, *Abcb1a/1b;Abcg2*^{-/-}, *Cyp3a*^{-/-} and *Cyp3aXAV* mice 8 hr after oral administration of 10 mg/kg lorlatinib. Data are presented as mean ± SD (*n* = 5–7). **p* < 0.05; ***p* < 0.01; ****p* < 0.001 compared to wild-type mice.

(Figs. 4d and 4e). Similar results were obtained for lorlatinib accumulation (Fig. 4f Table 2). In contrast, the liver and lung distribution of lorlatinib were not noticeably affected by elacridar treatment (Supporting Information, Fig. 8). Of note, we did not observe any sign of spontaneous toxicity of lorlatinib in any of the mouse strains that we tested with oral lorlatinib at 10 mg/kg, either in the absence or in the presence of elacridar.

Collectively, these data indicate that oral elacridar treatment can extensively and specifically inhibit the activity of mouse *Abcb1* (and perhaps *Abcg2*) in the BBB and BTB, leading to markedly increased lorlatinib concentrations in the brain and testis. The lack of effect of elacridar on the brain and testis accumulation in the *Abcb1a/1b;Abcg2*^{-/-} mice further suggests that other uptake or efflux systems for lorlatinib

across the BBB and BTB were not noticeably affected by elacridar at this dose (Figs. 4af Table 2).

Discussion

In this study, we found that the third-generation ALK/ROS1 inhibitor lorlatinib is modestly transported *in vitro* by human ABCB1 and mouse *Abcg2*, but not detectably by human ABCG2. *In vivo*, upon oral administration to wild-type, *Abcb1a/1b*^{-/-}, *Abcg2*^{-/-} and *Abcb1a/1b;Abcg2*^{-/-} mice, lorlatinib was rapidly and readily absorbed in all strains, without detectable differences in plasma AUC. However, the brain accumulation of lorlatinib was fourfold increased in both *Abcb1a/1b*-deficient strains, but not in the single *Abcg2*-deficient strain. This indicates that ABCB1/P-glycoprotein in the BBB can still markedly restrict the brain penetration of

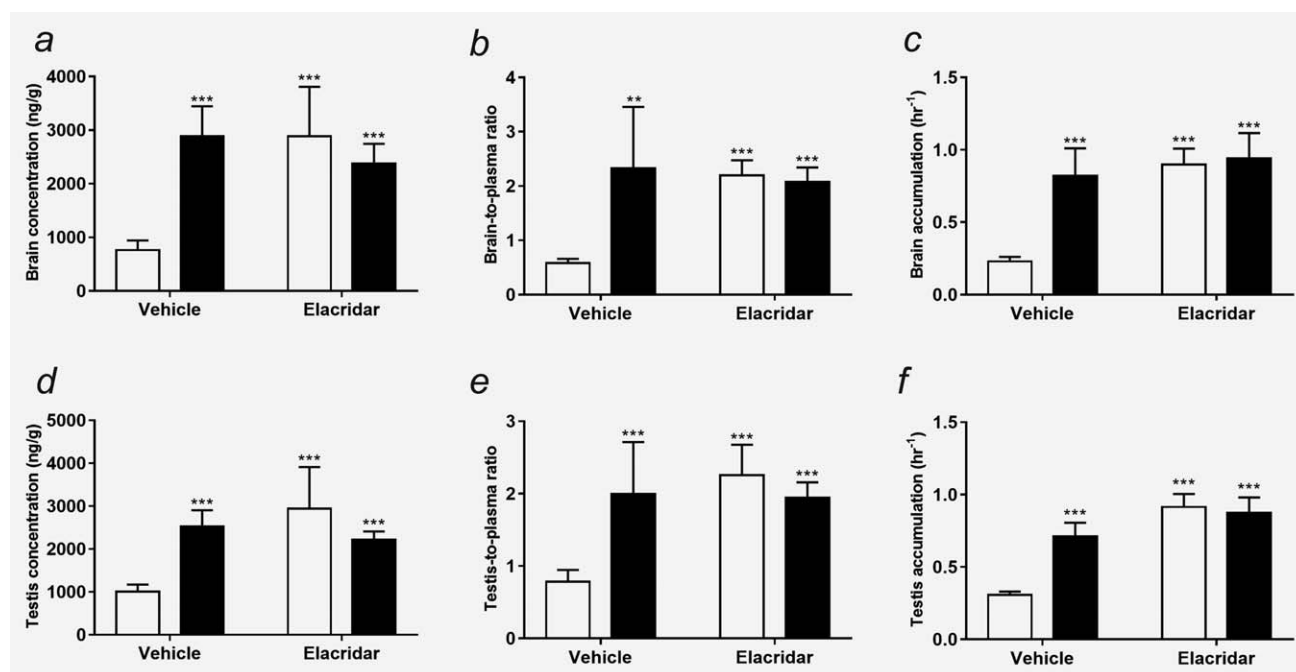


Figure 4. Brain and testis concentrations (a, d), tissue-to-plasma ratios (b, e) and tissue accumulations (c, f) of lorlatinib in male wild-type (white bars) and *Abcb1a/1b;Abcg2*^{-/-} mice (black bars) 2 hr after oral administration of 10 mg/kg lorlatinib without or with elacridar (100 mg/kg) co-administration. Data are presented as mean \pm SD ($n = 4-6$). * $p < 0.05$; ** $p < 0.01$; *** $p < 0.001$ compared to vehicle-treated wild-type mice.

Table 2. Plasma, brain and testis pharmacokinetic parameters of lorlatinib 2 hr after oral administration of 10 mg/kg lorlatinib to male wild-type and *Abcb1a/1b;Abcg2*^{-/-} mice with vehicle or elacridar coadministration

Parameter	Genotype and type of pretreatment			
	Vehicle		Elacridar	
	Wild-type	<i>Abcb1a/1b;Abcg2</i> ^{-/-}	Wild-type	<i>Abcb1a/1b;Abcg2</i> ^{-/-}
AUC _{0-2 hr} , ng/ml hr	3,305 \pm 515	3,620 \pm 818	3,264 \pm 1,141	2,555 \pm 309
Fold change AUC _{0-2 hr}	1.0	1.1	1.0	0.8
C _{max} , ng/ml	1,963 \pm 300	2,223 \pm 645	1,914 \pm 735	1,598 \pm 382
T _{max} , hr	0.5	0.5	0.5	0.5
C _{brain} , ng/g	764 \pm 177	2,888 \pm 558***	2,885 \pm 925***	2,379 \pm 366***
Fold increase C _{brain}	1.0	3.8	3.8	3.1
Brain-to-plasma ratio	0.58 \pm 0.08	2.33 \pm 1.13**	2.20 \pm 0.28***	2.08 \pm 0.26***
Fold increase ratio	1.0	4.0	3.8	3.6
P _{brain} ($\times 10^{-3}$ hr ⁻¹)	229.8 \pm 31.2	821.4 \pm 188.8***	897.6 \pm 110.8***	941.4 \pm 174.6***
Fold increase P _{brain}	1.0	3.6	4.0	4.1
C _{testis} , ng/g	1,011 \pm 160	2,525 \pm 381***	2,945 \pm 970***	2,214 \pm 195***
Fold increase C _{testis}	1.0	2.5	2.9	2.2
Testis-to-plasma ratio	0.79 \pm 0.16	2.00 \pm 0.72**	2.26 \pm 0.42***	1.94 \pm 0.22***
Fold increase ratio	1.0	2.5	2.9	2.5
P _{testis} ($\times 10^{-3}$ hr ⁻¹)	306.6 \pm 24.5	711.6 \pm 94.6***	914.3 \pm 90.0***	873.9 \pm 106.4***
Fold increase P _{testis}	1.0	2.3	3.0	2.8

Data are presented as mean \pm SD ($n = 4-6$). Lorlatinib was administered alone or coadministered with 100 mg/kg oral elacridar 15 min prior to lorlatinib administration. AUC_{0-2 hr}, area under plasma concentration-time curve; C_{max}, maximum concentration in plasma; T_{max}, time point (hr) of maximum plasma concentration; C_{brain/testis}, brain/testis concentration; P_{brain/testis}, brain/testis accumulation. * $p < 0.05$; ** $p < 0.01$; *** $p < 0.001$ compared to vehicle-treated wild-type mice.

lorlatinib. Qualitatively similar results were found for the testis. In contrast, all other tested tissues, that lack a distinct blood–tissue barrier, were not noticeably affected by the transporter deficiencies. This P-glycoprotein-mediated restriction of brain and testis accumulation of lorlatinib could be fully reversed by oral coadministration of elacridar. We further found that lorlatinib oral availability in mice was markedly restricted by mouse Cyp3a and especially human CYP3A4, indicating that CYP3A can play a substantial role in the metabolic clearance of lorlatinib.

Given the importance of readily reaching brain metastases in treatment-resistant NSCLC, much attention was given during the development of lorlatinib to achieve high intrinsic membrane permeability, and minimal interaction with BBB efflux transporters like ABCB1 (P-glycoprotein) and ABCG2.⁹ These properties would likely result in comparatively easy passage of the drug across the BBB, which should allow the drug to reach high-level and extensive exposure of all tumor cells in brain metastases. While we find indeed relatively good brain penetration of lorlatinib in wild-type mice, with a brain-to-plasma ratio of about 0.5–0.6, this penetration could be enhanced another fourfold by removing or inhibiting P-glycoprotein in the BBB. Still, the wild-type brain values compare favorably to earlier generation ALK inhibitors. First-generation crizotinib showed a brain-to-plasma ratio of about 0.2 in wild-type mice, which could be enhanced 15-fold by removing or inhibiting P-glycoprotein.¹⁷ Second-generation ceritinib showed a brain-to-plasma ratio of 0.02 in wild-type mice, which could be enhanced >100-fold by removing or inhibiting P-glycoprotein and ABCG2.¹⁸ Indeed, early and, in part, anecdotal clinical evidence (including case reports) suggests that lorlatinib is quite effective against brain metastases in NSCLC and some other cancers as well, even after earlier generation ALK inhibitors failed.^{12,25,26} Ongoing Phase III clinical trials will systematically address this important aspect of lorlatinib in greater detail.¹² Nonetheless, even if there is still some clear *in vivo* interaction of lorlatinib with P-glycoprotein, early indications are that the effort to minimize these interactions and optimize intrinsic membrane permeability of the drug may have paid off in terms of improved brain accumulation. In addition, the chance that tumor cells that intrinsically express modest levels of P-glycoprotein will become markedly resistant to lorlatinib seems low.

In case it turns out that there is further benefit to be gained from enhancing lorlatinib accumulation in brain metastases or directly in tumor cells, the use of elacridar can be considered, also in view of the fact that this inhibitor did not noticeably affect the oral availability of lorlatinib, at least

in mice. In this context it is important to note that the plasma exposure level of elacridar used in our study is achievable in humans, as demonstrated by Kemper *et al.* (2001), who showed that a patient receiving 1000 mg of elacridar orally had almost the same elacridar plasma concentrations as mice treated with 100 mg/kg of elacridar orally.²⁷ We did not observe any sign of acute lorlatinib toxicity in wild-type or *Abcb1a/1b;Abcg2*^{-/-} mice, either with or without elacridar treatment. This suggests that oral coadministration of elacridar and lorlatinib may be considered to further improve the therapeutic efficacy against brain metastases and also primary brain tumors, without inducing systemic toxicity.

To date, very little information is publicly available on the possible interaction of lorlatinib with CYP3A. Our *in vivo* data in mice clearly indicate that both mouse Cyp3a and especially human CYP3A4 can substantially reduce the oral availability and thus overall body exposure of lorlatinib, whereas the relative tissue distribution of the drug was not much affected. This suggests that the metabolic clearance and oral availability of lorlatinib will likely be noticeably affected by CYP3A activity in patients as well. Looking ahead for broader clinical use of this drug, this will probably be an element that will need to be considered in the clinical dosing of lorlatinib. Still, our data suggest a moderate *in vivo* interaction of lorlatinib with CYP3A, rather than a very strong interaction. Like for many other drugs that are modestly affected by CYP3A activity, this will probably mean that coadministration of strong CYP3A-inducing or -inhibiting drugs with lorlatinib should be avoided or critically monitored.

To the best of our knowledge, this is the first study documenting that lorlatinib is significantly transported by both ABCB1 and ABCG2 *in vitro* and that in mice its brain accumulation, but not oral availability, is primarily restricted by ABCB1 (P-glycoprotein). Furthermore, human CYP3A4 and mouse Cyp3a can substantially restrict the oral availability of lorlatinib, without altering its relative tissue distribution. Coadministration of elacridar could markedly improve the brain and testis accumulation of oral lorlatinib without altering systemic exposure. The obtained insights and principles may be used to further enhance the therapeutic application and efficacy of lorlatinib, especially against brain metastases in NSCLC patients.

Acknowledgement

The authors thank Stéphanie van Hoppe for instructions in setting up the transwell transport assay and help in executing the *in vivo* mouse experiments.

References

1. Siegel RL, Miller KD, Jemal A. Cancer statistics, 2018. *CA Cancer J Clin* 2018.
2. Ettinger DS, Akerley W, Bepler G, et al. Non-small cell lung cancer. *J Natl Compr Canc Netw*. 2010;8:740–801.
3. Larsen JE, Cascone T, Gerber DE, et al. Targeted therapies for lung cancer: clinical experience and novel agents. *Cancer J (Sudbury, MA)* 2011;17:512–27.
4. Grande E, Bolos MV, Arriola E. Targeting oncogenic ALK: a promising strategy for cancer treatment. *Mol Cancer Therap* 2011;10:569–79.
5. Toyokawa G, Seto T. Updated evidence on the mechanisms of resistance to ALK inhibitors and strategies to overcome such resistance: clinical

- and preclinical data. *Oncol Res Treat* 2015;38:291–8.
6. Costa DB, Shaw AT, Ou SH, et al. Clinical experience with crizotinib in patients with advanced ALK-rearranged non-small-cell lung cancer and brain metastases. *J Clin Oncol* 2015;33:1881–8.
 7. Friboulet L, Li N, Katayama R, et al. The ALK inhibitor ceritinib overcomes crizotinib resistance in non-small cell lung cancer. *Cancer Disc* 2014;4:662–73.
 8. Metro G, Passaro A, Lo Russo G, et al. Ceritinib compassionate use for patients with crizotinib-refractory, anaplastic lymphoma kinase-positive advanced non-small-cell lung cancer. *Future Oncol (London, England)* 2018;14:353–61.
 9. Johnson TW, Richardson PF, Bailey S, et al. Discovery of (10R)-7-amino-12-fluoro-2,10,16-trimethyl-15-oxo-10,15,16,17-tetrahydro-2H-8,4-(metheno)pyrazolo[4,3-h][2,5,11]-benzoxadiazacyclo-tetradecine-3-carbonitrile (PF-06463922), a macrocyclic inhibitor of anaplastic lymphoma kinase (ALK) and c-ros oncogene 1 (ROS1) with pre-clinical brain exposure and broad-spectrum potency against ALK-resistant mutations. *J Med Chem* 2014;57:4720–44.
 10. Zou HY, Friboulet L, Kodack DP, et al. PF-06463922, an ALK/ROS1 inhibitor, overcomes resistance to first and second generation ALK inhibitors in preclinical models. *Cancer Cell* 2015;28:70–81.
 11. Shaw AT, Bauer TM, Felip E, et al. Clinical activity and safety of PF-06463922 from a dose escalation study in patients with advanced ALK+ or ROS1+ NSCLC. *J Clin Oncol* 2015;33:8018.
 12. Shaw AT, Felip E, Bauer TM, et al. Lorlatinib in non-small-cell lung cancer with ALK or ROS1 rearrangement: an international, multicentre, open-label, single-arm first-in-man phase 1 trial. *Lancet Oncol* 2017;18:1590–99.
 13. Shaw AT, Friboulet L, Leshchiner I, et al. Resensitization to crizotinib by the lorlatinib ALK resistance mutation L1198F. *N Engl J Med* 2016;374:54–61.
 14. Borst P, Elferink RO. Mammalian ABC transporters in health and disease. *Annu Rev Biochem* 2002;71:537–92.
 15. Agarwal S, Hartz AM, Elmquist WF, et al. Breast cancer resistance protein and P-glycoprotein in brain cancer: two gatekeepers team up. *Curr Pharma Des* 2011;17:2793–802.
 16. Schinkel AH, Jonker JW. Mammalian drug efflux transporters of the ATP binding cassette (ABC) family: an overview. *Adv Drug Deliv Rev* 2003;55:3–29.
 17. Tang SC, Nguyen LN, Sparidans RW, et al. Increased oral availability and brain accumulation of the ALK inhibitor crizotinib by coadministration of the P-glycoprotein (ABCB1) and breast cancer resistance protein (ABCG2) inhibitor elacridar. *Int J Cancer* 2014;134:1484–94.
 18. Kort A, Sparidans RW, Wagenaar E, et al. Brain accumulation of the EML4-ALK inhibitor ceritinib is restricted by P-glycoprotein (P-GP/ABCB1) and breast cancer resistance protein (BCRP/ABCG2). *Pharmacol Res* 2015;102:200–7.
 19. Katayama R, Sakashita T, Yanagitani N, et al. P-glycoprotein mediates ceritinib resistance in anaplastic lymphoma kinase-rearranged non-small cell lung cancer. *EBioMedicine* 2016;3:54–66.
 20. Thelen K, Dressman JB. Cytochrome P450-mediated metabolism in the human gut wall. *J Pharm Pharmacol* 2009;61:541–58.
 21. Paine MF, Hart HL, Ludington SS, et al. The human intestinal cytochrome P450 “pie”. *Drug Metab Dispos Biol Fate Chem* 2006;34:880–6.
 22. Spatari C, Li W, Schinkel AH, et al. Bioanalytical assay for the quantification of the ALK inhibitor lorlatinib in mouse plasma using liquid chromatography-tandem mass spectrometry. *J Chromatogr B Analyt Technol Biomed Life Sci* 2018;1083:204–08.
 23. Evers R, Kool M, van Deemter L, et al. Drug export activity of the human canalicular multispecific organic anion transporter in polarized kidney MDCK cells expressing cMOAT (MRP2) cDNA. *J Clin Invest* 1998;101:1310–9.
 24. Bakos E, Evers R, Calenda G, et al. Characterization of the amino-terminal regions in the human multidrug resistance protein (MRP1). *J Cell Sci* 2000;113:4451–61.
 25. Yuan C, Ma MJ, Parker JV, et al. Metastatic anaplastic lymphoma kinase-1 (ALK-1)-rearranged inflammatory myofibroblastic sarcoma to the brain with leptomeningeal involvement: favorable response to serial ALK inhibitors: a case report. *Am J Case Rep* 2017;18:799–804.
 26. Hochmair MJ, Schwab S, Prosch H. Complete remission of intrathecal metastases with lorlatinib therapy in a heavily pretreated ALK-positive lung cancer patient. *Anti-Cancer Drugs* 2017;28:928–30.
 27. Kemper EM, Jansen B, Brouwer KR, et al. Bioanalysis and preliminary pharmacokinetics of the acridonecarboxamide derivative GF120918 in plasma of mice and humans by ion-pairing reversed-phase high-performance liquid chromatography with fluorescence detection. *J Chromatogr B Biomed Sci Appl* 2001;759:135–43.

THE DIFFERENCE OF BREAKTHROUGH MOMENTS

WITH AN INTEGRATED SOLUTION FOR
GROUNDBREAKING SINGLE-CELL RESEARCH

BD Accuri™ C6 Plus Personal Flow Cytometer

BD FACSCelesta™ Cell Analyzer

BD LSRFortessa™ X-20 Cell Analyzer

BD FACSMelody™ Cell Sorter

FlowJo™ Software

One of the largest portfolios of reagents

Discover more >

